Minimization of Friction Influence on the Evaluation of Rheological Parameters From Compression Test: Application to a Forging Steel Behavior Identification

S. Diot

D. Guines
e-mail: dominique.guines@insa-rennes.fr

A. Gavrus

E. Ragneau

Laboratoire de Génie Civil et Génie Mécanique
(LGCGM), EA 3913,
National Institute of Applied Sciences (INSA),
20 Avenue des Buttes de Coësmes, CS 14315,
35043 Rennes Cédex, France

In order to characterize the metal behavior at strain, strain rate, and temperature range encountered in metal forming processes, the rheological compressive test is well adapted and has been often used. Nevertheless, this experimental test is more complicated to realize than the extension one and requires some particular considerations owing to the friction condition occurring between the specimen and the dies. This paper deals with a new specimen shape proposed to realize both static and dynamic compression tests. The independence of the material parameters to die friction is highlighted by means of a pseudo-experimental validation. The proposed specimen shape is validated by compression tests carried out on a 50CD4 steel (norm EN 10 083). The choice of the mathematical form of the constitutive law allowing to characterize its behavior at strains, strain rates, and temperatures corresponding to an extrusion application is then discussed. To replicate more accurately the nonuniformity of the different fields in the specimen, a classical inverse procedure consisting in coupling a finite element model of the compression test with an optimization module is used to determined the rheological parameters.
[DOI: 10.1115/1.3026543]

Keywords: friction, compression, rheological behavior, inverse analysis, finite element simulation, dynamic

1 Introduction

In recent years, finite element method (FEM) simulations have been extensively used for the development and optimization of metal forming processes. To obtain accurate results within these simulations, material models and their input data are needed. The implementation of these material models into finite element (FE) packages is commonly realized through constitutive relationships which describe, into one single equation, the plastic behavior of materials as a function of strain, strain rates, and temperature. The most common way to evaluate the parameters of these constitutive models is based on performing tests on specimens. Many metallic alloys, used in forming applications, are subjected to strain and viscoplastic hardening when the plastic deformation process occurs. Viscoplasticity implies a strain rate dependency, which becomes significant when the strain rate reaches a value around 10 s^{-1} [1,2]. The strain hardening is easily obtained by submitting the material to static loading by means of a conventional testing machine. On the other hand, the characterization of the viscoplastic hardening requires some particular considerations owing to dynamic loadings which have to be applied to material samples. An overview of rheological laws developed and of general experimental tests reveals that there is a lack of characterization methods dedicated to intermediate strain rates range, up to 500 s^{-1}, encountered in forming applications [3]. As far as forging and metal forming are concerned, tensile, torsion, and compression tests have been extensively used in order to characterize the thermo-elasto-viscoplastic behavior of the material. The tensile test is widely used although the plastic instability and the strain localization (necking phenomenon) [4] which appear at the maximum load do not allow the characterization of the material behavior at large strains. Torsion test has often been used since large strains (600–800%) can then be reached. Finally, the compression test has the advantage of generating sollicitations suitable to forming applications and sufficient strain levels (up to 150%). From an experimental point of view, the compression test is more complicated to realize than the traction one. The main difficulties encountered in realizing a compression test are ensuring the coaxiality of the forces applied on the specimen faces to avoid shearing and considering the friction that appears between the sample and the tools, particularly for tests carried out at intermediate or high strain rates and elevated temperature ranges [5]. Usually, the specimen geometry is cylindrical and a uniform strain field is assumed in the whole specimen, the displacement ΔL and the force $F^{\exp}$ measurements allow to compute, respectively,

- the true stress

$$\bar{\sigma} = \frac{F^{\exp}}{S_0}\frac{L_0 - \Delta L}{L_0} \tag{1}$$

  where L_0 and S_0 are, respectively, the initial length and initial section of the specimen,
- the true strain

$$\bar{\varepsilon} = \ln[L_0 - \Delta L/L_0] \tag{2}$$

  When the test is realized at a velocity V, the strain rate is then given by

Contributed by the Materials Division of ASME for publication in the JOURNAL OF ENGINEERING MATERIALS AND TECHNOLOGY. Manuscript received January 17, 2007; final manuscript received August 18, 2008; published online December 15, 2008. Assoc. Editor: Mohammed Cherkaoui.

Copyright © 2009 by ASME

Downloaded From: http://materialstechnology.asmedigitalcollection.asme.org/ on 09/29/2013 Terms of Use: http://asme.org/terms

$$\dot{\bar{\varepsilon}} = V/(L_0 - \Delta L) \tag{3}$$

From these "experimental" results a rheological law $\bar{\sigma} = f(\bar{\varepsilon}, \dot{\bar{\varepsilon}}, T, \ldots)$ can be identified, where T is the temperature. However, the friction between die-specimen interfaces generates barreling [6] and stress, and strain fields are no longer uniform in the specimen. To reduce the effect of friction, efforts have been made in the past in order to define an appropriate specimen shape (double-cup specimen, narrow-neck specimen, Rastegaev specimens, etc.). In spite of these efforts, the influence of friction on forming processes still remains a problem. Special attention has been given to friction losses and to the corresponding friction conditions. Van Rooyen and Backoffen [7] measured the frictional stress at the interfaces when compressing aluminum cylinders using flat dies. For cylinders with a height-to-diameter ratio equal to 0.25 and for a maximum height reduction of 40%, the frictional stress was constant when sheets of lead were placed at the interfaces, increased linearly from the center to the circumference when the dies were unlubricated, first increased with the radius and then remained constant when the dies were oil lubricated, and decreased during the test when molybden bisulphide additive was used. Oh and Kobayashi [8] took into account experimental data relating the normal pressures at the interface to calculate the frictional stress distribution when upsetting aluminum alloy cylinders, with either unlubricated or lubricated conditions. In the first case, the distribution of the frictional shear stress was uniform for small reductions, but varied for larger reductions. In the second case, the distribution was fairly uniform. Gelin et al. [9] proposed a new procedure for obtaining accurate stress-strain characteristics from the axisymmetric upsetting of solid cylinders of 1.5 height-to-diameter ratio.

A new upper bound analysis has been developed to predict metal flow. The friction stress at the die-cylinder interface has been assumed to increase linearly from the center of the cylinder to the circumference. The predicted profiles of the bulging cylindrical surfaces are nearly the same as those observed experimentally up to a height reduction of 50%.

For the quantitative evaluation of friction, ring compression test is a typical method in metal forming. It was first proposed by Kunogi [10] and was later improved by Male and Cockcroft [11]. A number of works, both experimental and theoretical, showed the usefulness of this method in determining friction at the die-workpiece interface for isotropic materials. The upper bound solution by Avitzur [12] has been widely used to infer theoretical friction factors [13–15]. However, Avitzur's solution was not able to model barreling or "bulging" of the specimen. In order to asssess Avitzur's theoretical solution, Male and de Pierre [15] conducted ring compression test using strain rates between 10 s^{-1} and 10^2 s^{-1}. The correlation between theoretical and experimental results was generally good, but a tendency of the analysis to overestimate theoretical friction factors was noted. Various attemps have been made to improve on the available theoretical solutions by employing assumptions that better approximate observed ring behavior [16–18]. An assessment of the available solutions by Rao and Sivaram [16] indicates that the more advanced theoretical solutions that incorporate barreling, such as those by Liu [17] and the upper-bound approach by Lee and Altan [18], produce results similar to those of Avitzur's analysis. Agreement is very good at low strains and for low friction, as discussed by Hwu et al. [19].

As one can see, conventional interpretation of the test results is then often difficult. Different approaches are encountered to treat this problem. The first one consists in minimizing the friction by using a lubrication device. Some authors propose to use tools or specimens with a specific geometry (Rastegaev geometry) allowing to constrain the lubricant in the sliding face [20–22]. This treatment enables converting the measured values $(\Delta L, F^{\exp})$ into local values (true strain, true stress). The advantage of this first method is the possibility of calculating the stress-strain state in the sample directly from the force and the displacement measured during the compression test by means of the relationships given by Eqs. (1) and (2), the so-called analytical model. However, friction is difficult to eliminate and is still a difficulty that harms the accuracy of the rheological parameters' identification. A second approach is to maximize friction in order to obtain sticking conditions [23]. This method is often used for hot temperature tests: Indeed, to eliminate friction in those operating conditions is even more difficult. The main advantage of this method is that the test can be performed with a high level of reproducibility. In this case, numerical models are required for calculating the inhomogeneous stress-strain state in the sample. Nowadays, numerical approaches are used more and more. The numerical models are mostly based on the FEM and are extensively used in combination with optimization methods in so-called inverse analysis procedures to identify the parameters of rheological laws from experimental tests [24,25,4,49], Fig. 1. Besides, with a finite element model, it is no longer necessary to realize tests with homogeneous deformation since it is possible to work with the values directly measured (force and displacement) instead of the local values of true strain and true stress (which are unknown). Based on these inverse methods coupling FEM calculations and optimization techniques, Szyndler and et al. [26] evaluated both friction coefficients and rheological parameters from the results of a hot ring compression test. Szeliga et al. [27] performed axisymmetric compression and plane-strain compression tests on specimens of carbon-manganese steeel. Die-specimen interfaces were lubricated to decrease friction in tests. The friction coefficient was determined on the basis of additional ring compression tests. It was shown that the flow stress sensitivity to the test conditions is negligible when the inverse method is applied to the interpretation of the tests' results. In a similar way, Gavrus et al. [28] proposed to identify rheological parameters and friction coefficients directly from forging processes as, for example, a cylindrical upsetting and a direct extrusion.

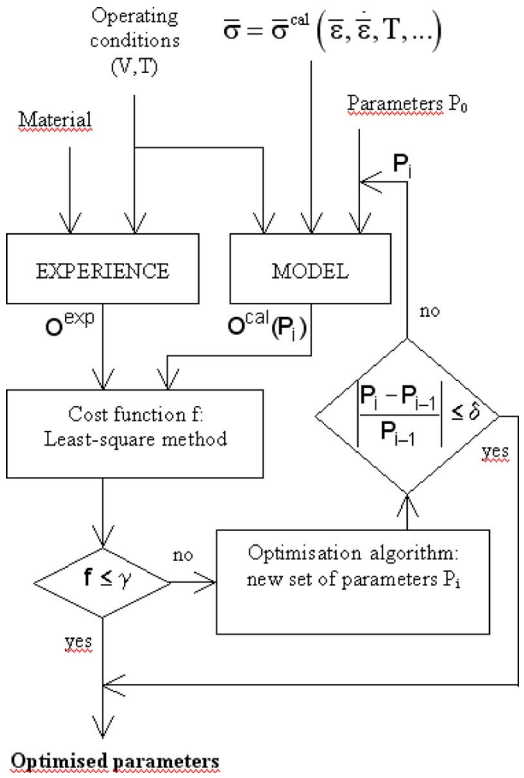

Fig. 1 Inverse analysis: rheological parameter characterization by iterative procedure

Downloaded From: http://materialstechnology.asmedigitalcollection.asme.org/ on 09/29/2013 Terms of Use: http://asme.org/terms

Table 1 Analysis of rheological experimental tests from analytical and numerical models

	Model	
	Analytical	Numerical
Experimental: O^{exp}	$F^{exp}(\Delta L, V, T)$ ⇓ Analytical model ⇓ $\bar{\sigma}^{exp}(\bar{\varepsilon}, \dot{\bar{\varepsilon}}, T)$	$F^{exp}(\Delta L, V, T)$
Calculation: $O^{cal}(P)$	$\bar{\sigma}^{cal}(P, \bar{\varepsilon}, \dot{\bar{\varepsilon}}, T)$	$\bar{\sigma}^{cal}(P, \bar{\varepsilon}, \dot{\bar{\varepsilon}}, T)$ ⇓ Numerical model ⇓ $F^{cal}(P, \Delta L, V, T)$
f	$f(\bar{\sigma}^{exp}, \bar{\sigma}^{cal}(P))$	$f(F^{exp}, F^{cal}(P))$

Whatever the method used, optimization technics, which are iterative procedures, are necessary to identify the constants of the constitutive law. Table 1 introduces these iterative procedures for both analytical and numerical models. The parameters P of the constitutive law are the ones that minimize the deviation—expressed by a least-square function f—between the observable experimental variable O^{exp} and the observable calculated one $O^{cal}(P)$. $\bar{\sigma}^{exp}$ and $\bar{\sigma}^{cal}$ are, respectively, the true stress obtained by Eq. (1) and the true stress calculated from the set of material parameters P.

The general framework of this study is the thermoviscoplastic behavior characterization of materials encountered in forming applications. The principal aim of this work is to propose a new specimen shape allowing (a) the identification of the coefficients of the constitutive law independently from friction between the specimen and the tools, and (b) the protection of the load cell against overloads in the case of dynamic tests. Through numerical FE simulations of the compression test, different specimen shapes have been investigated. In this paper, results are presented for the classical shape (cylindrical) and for the proposed one, so-called dumbbell specimen shape. To confirm the independence of the constitutive law parameters from friction that develops between the specimen and the dies, a pseudo-experimental study is realized and the interest of the chosen specimen shape to realize dynamic compression tests is shown. Then, compression tests are performed on 50CD4 steel specimens in order to characterize its behavior at temperatures between 298 K and 673 K and at strains and strain rates achieved in a specific extrusion application. The choice of the mathematical formulation of the constitutive law describing the evolution of the Von Mises flow stress as a function of the generalized strain, the generalized strain rate, and the temperature is discussed. Experimental load-displacement diagrams are then used to identify the constitutive law parameters by means of an automatic inverse procedure consisting in coupling a finite element model of the compression test with an optimization module.

2 Specimen Geometry

Classical samples used to perform compression tests are cylindrical. At high temperatures, the minimization of friction by an appropriate lubrication device seems not easy to realize and may not be sufficient to ensure full sliding conditions at the specimen/tools interfaces. Also, the nonuniformity of the different fields (strain, strain rate, stress, and temperature) requires the use of an inverse procedure to identify the rheological parameters. Nevertheless, the direct FE model of the compression test used in this procedure requires knowing the values of the friction coefficient at tools/specimens interfaces. Unfortunately, the latter is not exactly known. Moreover, to realize dynamic tests at intermediate or high strain rates, the actuator displacement rate requires taking extra care in order to avoid an overload of the sensor at the end of the compression stage, when the stiffness of the specimen becomes very important.

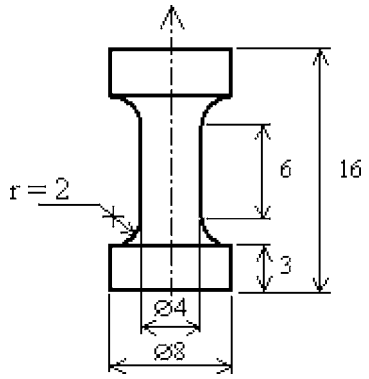

Fig. 2 Dimensions (in millimeter) of the compression specimen

In order to minimize the friction dependence of the material parameters, we have to increase the localization of the strains in the middle of the specimen as far as possible from the interfaces. However, the critical length leading to the apparition of buckling limits the choice of the specimen height. The diameter of the cylindrical specimen is defined by the maximum load capacity of the experimental device and also by the maximum strength of the tested material. François [29] recommends a height-to-diameter (H/D) ratio of 3, where H is the height and D the diameter of the specimen, but in literature a ratio $H/D=1.5$ is commonly adopted in order to avoid the apparition of a double barrel [30–32]. Considering both the capacity of the hydraulic machine used to realize the experimental tests and the nature of the tested material, different shapes have been investigated by means of FE modeling of the sample compression. "Heads" have been added to the "classical" cylindrical specimen in order to isolate the deformed part from the friction area at the interface between specimen and tools. The proposed shape, called dumbbell specimen, is introduced in Fig. 2. This shape allows us to concentrate the plastic strain in the middle of the specimen (a cylinder with a ratio of 1.5), as shown Fig. 5. The heads are dimensioned to remain elastic throughout the test. This kind of sample has been used previously in split Hopkinson pressure bar devices [33]. Moreover, the total height of 16 mm of this particular shape compared to the 6 mm height of the classical one makes it possible for the actuator to stop without generating a too significant overload that would be dangerous for the load cell. As one can see in Fig. 6, the measured load do not exceed 20 kN on a dumbbell specimen (the maximum dynamic capacity of the machine) for a 4 mm length compression, whereas a classical cylindrical specimen leads to 40 kN force on the load sensor.

Another difficulty encountered in realizing a compression test is ensuring that the forces applied on the specimen faces remain coaxial during the test to avoid the appearance of shearing. In order to do this a special device, similar to a tube, fixed on the load sensor has been designed (Fig. 3). The specimen is impacted by the actuator rod via an intermediate tool which remains coaxial with the specimen for the duration of the compression test [3]. The design of the servohydraulic testing machine ensures a good coaxiality between the load cell and actuator rod axis. The coaxiality between the intermediate tool and the specimen is ensured by an appropriate diametral gap (less than 0.01 mm) between the

Downloaded From: http://materialstechnology.asmedigitalcollection.asme.org/ on 09/29/2013 Terms of Use: http://asme.org/terms

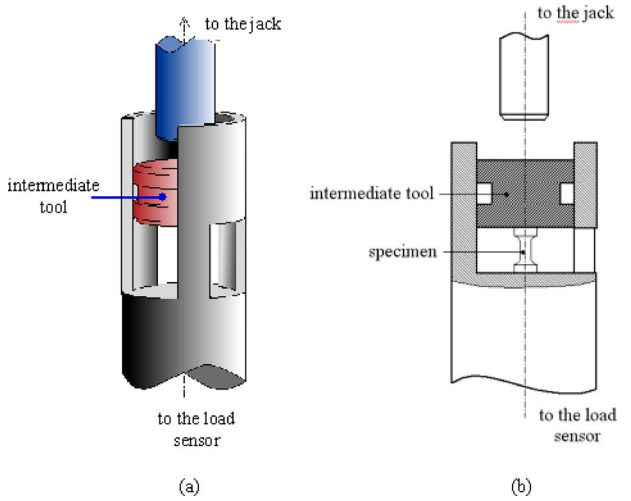

Fig. 3 Experimental compression device: (*a*) 3D view without specimen, and (*b*) view cut with specimen

tube and the intermediate tool. The flat smooth intermediate tool end faces are lapped to eight rms surface finish, with opposite faces parallel to within 5 μm over a diameter of 30 mm. The friction effect between the intermediate tool and tube is minimized by the combination of hard, smooth parts, lubricant well geometry, and glass lubricant, which provided excellent lubrication.

3 Compression Test Model

In order to study what happens in the dumbbell specimen during compression, a finite element model of the test is developed. A thermo-elasto-viscoplastic behavior of the specimen material is considered. The rheological law is assumed to be as follows:

$$\bar{\sigma} = K\bar{\varepsilon}^n \exp\left(\frac{\beta}{T}\right)\dot{\bar{\varepsilon}}^m \tag{4}$$

where $\bar{\sigma}$ is the Von Mises stress, $\bar{\varepsilon}$ is the generalized strain, and $\dot{\bar{\varepsilon}}$ is the generalized strain rate, with $K=500$ MPa, $n=0.2$, $m=0.05$ and $\beta=150$ K. The model takes into account the self-heating (temperature rise due to plastic work) of the material during compression. Considering the revolution shape of the specimen, an axisymmetric model is used. The specimen is meshed with six node triangles (Fig. 4).

The node's displacements on its lower face are fixed, whereas a constant velocity $V=3$ m s^{-1} is imposed on the upper face. The initial temperature of the sample and tools is 293 K. A Coulomb law describes the friction at the specimen/tools interfaces

$$\tau_c = \min(\mu\sigma_n, \sigma_0/\sqrt{3}) \tag{5}$$

with τ the tangent stress, σ_n the normal stress, and σ_0 the flow stress. Two cases are then defined:

- $\tau < \tau_c$, then sticking friction is considered
- $\tau = \tau_c$, then there is λ such as $V_g = -\lambda\tau$, where V_g is the sliding velocity

The finite element commercial package FORGE2® [34] is used to simulate the compression of the dumbbell specimen. Considering the friction coefficient $\mu=0.13$, the simulation shows that strain is localized in the middle part of the specimen (Fig. 5). These results (Figs. 5 and 6) have been obtained for an impactor velocity of 3 m s^{-1}, an initial strain rate of 500 s^{-1}, and an initial room temperature of 293 K. Instinctively one can think that friction at the specimen/tools interface has no influence on deformation.

Also, the influence of the friction coefficient value ($\mu=0.13$ and $\mu=0.3$, modeling, respectively, a lubricated and a dry contact) is evaluated. The FE numerical simulations are used to compare the load versus displacement curves for two values of the friction coefficient (Fig. 6). The comparison is extended to the compression tests made on standard cylindrical specimens ($D=4$ mm, $H=6$ mm). Figure 6 shows that the load versus displacement curves are not sensitive to friction coefficient for displacements up to 5.5 mm and 3.5 mm, respectively, for the dumbbell and cylindrical samples, which correspond to a maximum equivalent plastic strain of 150% for the dumbbell specimen and 60% for the cylindrical one. Moreover, these curves show the interest of this kind of geometry to protect the load sensor against an overload in the case of dynamic compression testing. Indeed, due to the more important height of the dumbbell sample and to the strain concentration in the central part of the specimen, a reduced force is applied on the load sensor to a given displacement level. Also, the actuator can be stopped without generating a too important overload on the load sensor.

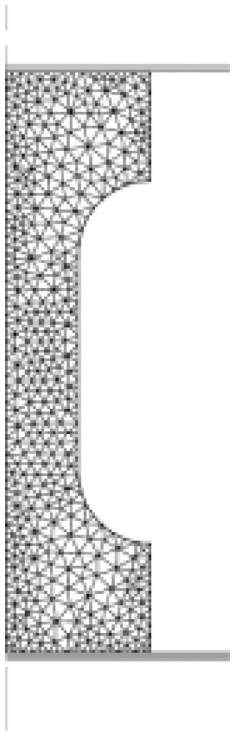

Fig. 4 Compression specimen mesh

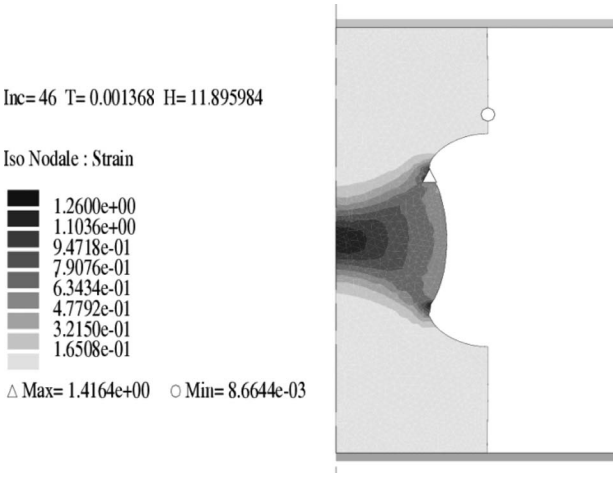

Fig. 5 Strain in the specimen during the compression test

Downloaded From: http://materialstechnology.asmedigitalcollection.asme.org/ on 09/29/2013 Terms of Use: http://asme.org/terms

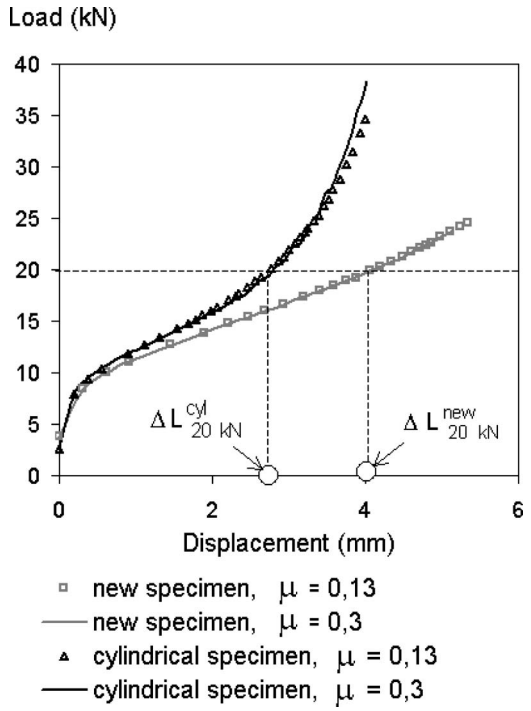

Fig. 6 Influence of friction coefficient on the compression force

The objective is not necessarily to minimize the friction, but to define a procedure able to identify the material parameters of the plastic rheological law independently of friction that develops between the specimen and the tools. Since the plastic rheological law describes the evolution of the Von Mises equivalent stress with respect to equivalent strain, generalized strain rate, and temperature, comparisons of these fields led to two friction coefficient values of 0.13 and 0.3. These comparisons are performed to two displacement values: the first one, $\Delta L^{\text{new}}_{20\text{ kN}}$, corresponds to a compression force of 20 kN (maximum force capacity of the machine), while the second one is $\Delta L^{\text{new}}_{20\text{ kN}}/2$. The deviation between the values obtained with the two friction coefficients is expressed by a function

$$D\ (\%) = 100 \times \left|(R_{\mu=0.13} - R_{\mu=0.3})/R_{\mu=0.13}\right| \tag{6}$$

where R is strain, strain rate, or temperature in the central point of the sample. The results are introduced in Tables 2 and 3.

Table 2 shows that the equivalent strain, the generalized strain rate, and the temperature fields are very sensitive to friction condition for cylindrical specimens. The deviation varies between

Table 2 Cylindrical specimens: influence of friction coefficient at tools/specimen interfaces on strains, strain rates, and temperatures in the heart of the specimen

	$\Delta L^{\text{new}}_{20\text{ kN}}/2$		$\Delta L^{\text{new}}_{20\text{ kN}}$	
	μ=0.13	μ=0.3	μ=0.13	μ=0.3
$\dot{\bar{\varepsilon}}$ (s^{-1})	1231	1430.3	1732.8	2608.6
D (%)	16.19%		50.54%	
$\bar{\varepsilon}$	0.4	0.459	1.1	1.374
D (%)	14.75%		24.91%	
T (K)	374.48	387.94	536.45	595.9
D (%)	13.26%		22.57%	

Table 3 Dumbbell specimens: influence of friction coefficient at tools/specimen interfaces on strains, strain rates, and temperatures in the heart of the specimen

	$\Delta L^{\text{new}}_{20\text{ kN}}/2$		$\Delta L^{\text{new}}_{20\text{ kN}}$	
	μ=0.13	μ=0.3	μ=0.13	μ=0.3
$\dot{\bar{\varepsilon}}$ (s^{-1})	852.8	856.07	1522.5	1463.3
D (%)	0.38%		3.89%	
$\bar{\varepsilon}$	0.417	0.418	1.226	1.233
D (%)	0.24%		0.57%	
T (K)	377.22	377.36	536.74	564.92
D (%)	0.13%		0.41%	

13% and 50% in the heart of the cylindrical specimen. On the contrary, Table 3 shows that for dumbbell specimens, the friction coefficient taken into account have an insignificant influence on these fields. The deviation varies between 0.13% and 4%. The local effect of friction on the sample heads, which remain elastic, does not modify the distribution of the strain, strain rate, and temperature fields in the central zone of the specimen. Since neither these fields nor the load versus displacement curves are sensitive to the value of friction coefficient for the dumbbell shape, one can think that it will be the same for the material identification of the parameters for the rheological plastic law.

4 Pseudo-Experimental Validation

In order to confirm the independence of material parameters identification to friction that develops between the specimen and the tools, a pseudo-experimental study is realized. The principle of this study is presented in Fig. 7. By means of the FE model defined above (Sec. 3), the compression of the specimen is simulated considering a Coulomb friction coefficient μ=0.13 at the tools/specimen interfaces to the following operating conditions:

- temperatures: 298 K, 473 K, and 673 K
- velocities: 3×10^{-4} m s^{-1} and 3×10^{-2} m s^{-1}

$P_{\text{init}}=\{K,n,\beta,m\}$ is the set of known parameters with K =500 MPa, n=0.2, β=150 K, and m=0.05. The six force versus displacement curves thus obtained make up the "pseudo-experimental" database. From this pseudo-experimental database an inverse procedure coupling the FE model of the compression test and an optimization tool is used (Fig. 1) to identify the set of parameters P_{iden} of the rheological law. The Coulomb friction coefficient considered at tools/specimen interfaces during the test is μ=0.3. The deviation between the parameters identified and the initial ones is expressed via the function

$$D\ (\%) = 100 \times \left|(P_{\text{init}} - P_{\text{iden}})/P_{\text{init}}\right| \tag{7}$$

The results are introduced in Table 4. The parameters identified are very close to the initial ones, the maximum deviation is obtained to the parameter n and is less than 3%. The comparison of the pseudo-experimental force versus displacement curves with those recalculated from the identified parameters is presented in Fig. 8. The good agreement between these results demonstrates the independence of the rheological parameter determination from friction tools/specimen interfaces and the relevance of the proposed specimen shape.

5 Example: Characterization of 50CrMo4 Steel Behavior

In the first part of this paper, a new specimen shape has been defined to realize compression tests which are used to identify plastic rheological laws encountered in forging applications. For

Downloaded From: http://materialstechnology.asmedigitalcollection.asme.org/ on 09/29/2013 Terms of Use: http://asme.org/terms

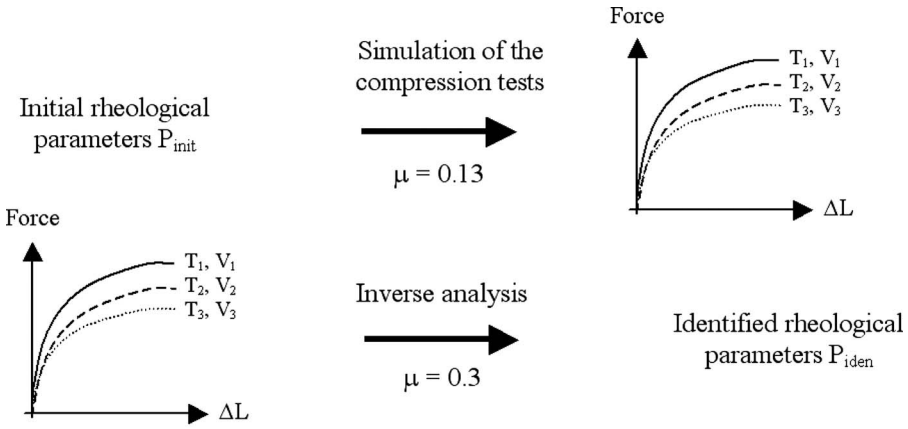

$$\text{Deviation}(\%) = 100 \times \frac{|P_{init} - P_{iden}|}{P_{init}}$$

Fig. 7 Numerical validation of the independence of the material characterization from die friction

the proposed shape, so-called dumbbell specimen, the independence of the rheological parameter identification from friction that develops between the specimen and the dies has been shown. In the second part of this paper, the proposed dumbbell shape is validated by means of compression tests performed at initial strain rates and temperatures corresponding to those encountered in an extrusion application. In this process, the considered material is worked at ambient temperature and only its self-heating leads to a temperature rise. For other forging applications, compression tests could be performed at higher strain rates and temperatures.

Experiments have been performed on dumbbell and cylindrical specimens, but only results on dumbbell specimens are used to identify the constitutive law since it has been shown through numerical investigations that friction between the specimen and the tools did not influence the fields of strain, strain rate, and temperature in the central part of the dumbell specimen.

Uniaxial compression tests are carried out on 50CrMo4 specimens using a computer-controlled servohydraulic testing machine. Its load capacity is 20 kN (dynamic) and 30 kN (static). As explained above, the friction between the specimen and the tools generates barreling and the stress and strain fields are no longer uniform in the specimen. Also, the rheological parameters of the constitutive law cannot be identified from the local variables such as strain and stress but from the two global variables measured during the tests, i.e., the displacement and the force. A linear variable differential transformer (LVDT) sensor set on the top of the actuator is used to measure displacement. The location and the accuracy of this displacement sensor do not make it possible to analyze the elastic response of the material. Therefore, only the inelastic part of the behavior will be studied. The elastic constants have been previously identified by means of an appropriate device. The stiffness of the setup is taken into account automatically by the software in order to not integrate the corresponding displacement to the one measured by the LVDT sensor. To characterize the plastic behavior, the plastic strains are calculated by means of Eq. (2). In this equation, displacements can be measured with a sufficient accuracy by the LVDT cross head sensor. As far as forging applications are concerned, the characterization of the material behavior at high strain level (up to 150%) allows to neglect the elastic displacements of the specimen compression. A conventional load cell (using resistive strain gages), fixed on the lower part of the machine, is used to measure the load. For high temperature tests, an electrical resistance tube furnace is mounted on the machine. The tools and their direct environment are held at a constant temperature during the measurement. The different operating conditions of these tests are the following:

- compression velocities: 3×10^{-4} m s^{-1} and 3×10^{-2} m s^{-1}, which correspond, respectively, to 5×10^{-2} s^{-1} and 5 s^{-1} initial strain rates
- Initial temperatures of the material: 298 K, 473 K, and

Table 4 Results of the pseudo-experimental validation

	P^{init}	P^{iden}	D (%)
K (MPa)	500	491.698	1.66
n	0.2	0.194081	2.96
m	0.05	0.050579	1.16
β (K)	150	150.957	0.638

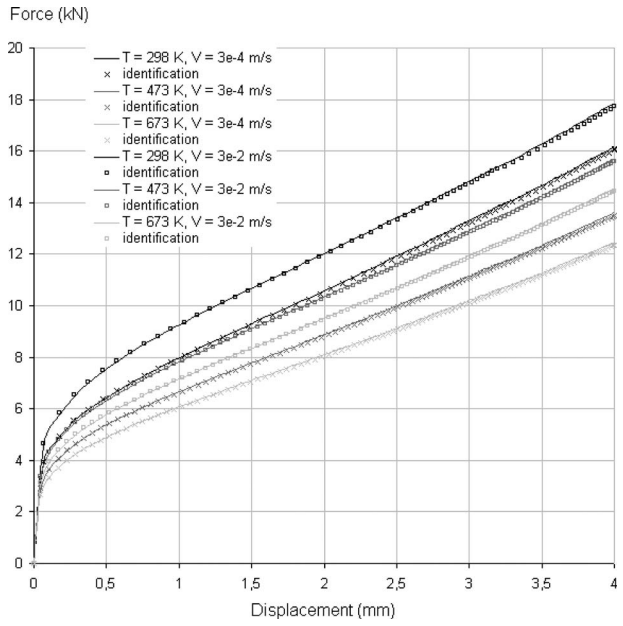

Fig. 8 Pseudo-experimental base and simulated curves from identified parameters

Downloaded From: http://materialstechnology.asmedigitalcollection.asme.org/ on 09/29/2013 Terms of Use: http://asme.org/terms

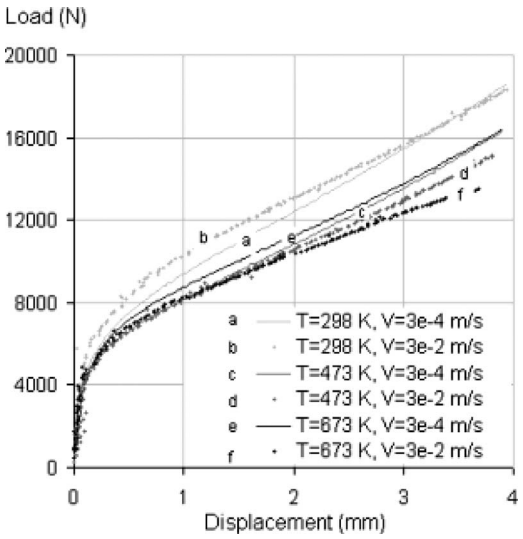

Fig. 9 Experimental load versus displacement curves for compression tests performed at speed *V* and temperature *T* on 50CrMo4 (EN 10 083) steel

673 K

The load versus displacement curves obtained are introduced in Fig. 9.

According to previous works in the field of forming and dynamic thermo-elasto-viscoplastic behavior, several additive [35,36] and multiplicative [37–40] constitutive equations have been used. Some models are devoted to a medium range of strain and strain rates [41,42], while others models are dedicated to an accurate description of the thermal softening [43,44]. An analysis of the present literature have shown that additive models are not good candidates for modeling the work-hardening behavior of materials with strong temperature and strain rate dependencies [45,46]. So plastic rheological laws, taking into account strain, strain rate, and temperature effects, are usually used in a multiplicative form to forming process simulations as follows [24]:

$$\bar{\sigma} = H(\bar{\varepsilon}, T) \times S(\dot{\bar{\varepsilon}}, T) \times \tau(T) \tag{8}$$

where H is a function describing work hardening and structural softening, S the strain rate sensitivity, and τ the influence of temperature.

The mathematical expressions of the different terms $H(\bar{\varepsilon}, T)$, $S(\dot{\bar{\varepsilon}}, T)$, and $\tau(T)$ are chosen in studying the equivalent stress evolution given by rheological tests. To do this, the load versus displacement curves are "converted" into "estimated stress" $\bar{\sigma}_{\text{est}}$ versus "estimated strain" $\bar{\varepsilon}_{\text{est}}$ (Fig. 10) by means of the analytical model previously introduced in Sec. 1 (Eqs. (1)–(3)) based on the assumption of homogeneous strain fields in the specimen to each initial strain rate and temperature. From an estimated strain $\bar{\varepsilon}_{\text{est}} = 0.3$, one can note a decrease of $\bar{\sigma}_{\text{est}}$. This evolution can be attributed to the softening of the material and also to the use of the classical analytical compression test model which does not correctly represent strain, strain rate, and temperature fields in the specimen for large deformations.

Figure 11 presents the maximal estimated stress $\bar{\sigma}_{\text{est}}^{\max}$ versus initial strain rate $\dot{\bar{\varepsilon}}_{\text{init}} = V/L_0$ for three different temperatures (298 K, 473 K and 673 K), where $L_0 = 6$ mm is the initial length of the central part of the specimen and V is the initial compression velocity. As one can see both in this figure and in Fig. 9, illustrating the load versus displacement curves, this material presents either a small positive or negative strain rate sensitivity depending on the considered temperature. So, this material does not exhibit significant strain rate sensitivity for the range of tested temperature and strain rate. This observation is in agreement with literature results [3,47,48] obtained for steels. So, in the constitutive equation (Eq. (8)) identified in this study, the strain rate sensitivity does not take into account ($S(\dot{\bar{\varepsilon}}, T) = 1$) for describing the behavior of this material for the tested operating conditions.

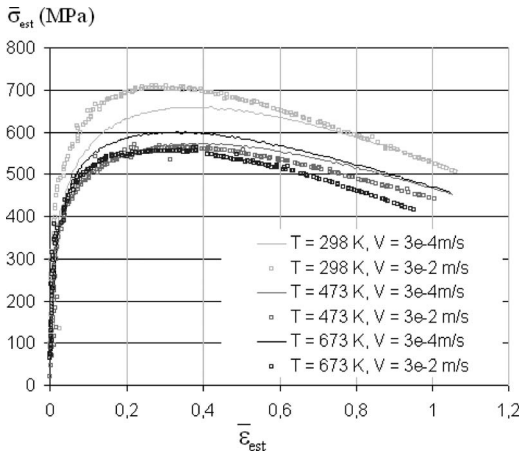

Fig. 10 Stress versus strain curves for compression tests performed at speed *V* and temperature *T* on 50CrMo4 (EN 10 083) steel

Classically, a power law $K\bar{\varepsilon}^{n(T)}$ is chosen to describe the work hardening influence of a steel. The evolution of $\ln(\bar{\sigma}_{\text{est}})$ versus $\ln(\bar{\varepsilon}_{\text{est}})$ to each tested temperature (Fig. 12) shows that the curves can be approached by lines that are almost parallel. The average of the different slopes gives an estimation of $n = 0.20463$. So, the strain-hardening exponent is not considered temperature dependent for the temperature range corresponding to this extrusion application. Concerning structural softening, it is difficult to evaluate the interest of modeling this behavior since the model used is not a good predicted one to strains larger than 0.3. Also, the law will be identified with and without a softening term $\exp(-r\bar{\varepsilon})$. The best results will then be kept. The influence of strain will then be modeled by

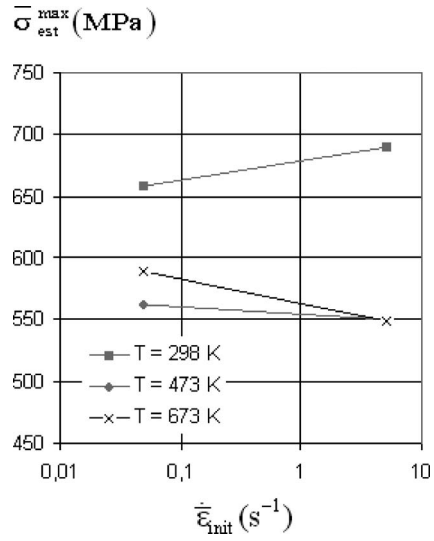

Fig. 11 Initial strain rate influence on the maximal estimated stress

Downloaded From: http://materialstechnology.asmedigitalcollection.asme.org/ on 09/29/2013 Terms of Use: http://asme.org/terms

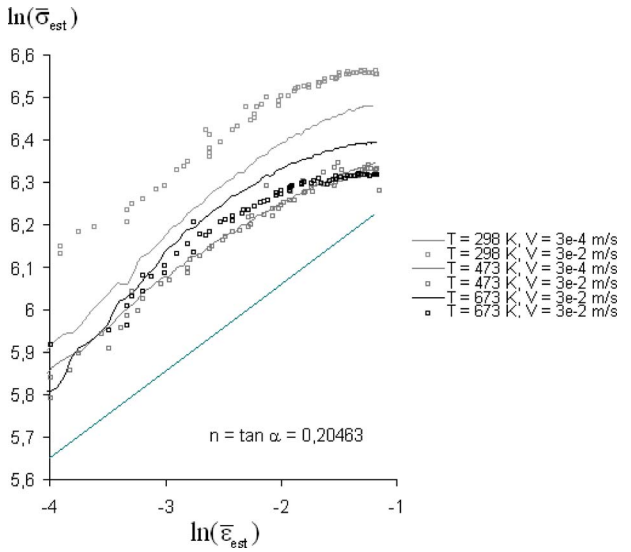

Fig. 12 Influence of strain

$$H(\bar{\varepsilon},T) = H(\bar{\varepsilon}) = K\bar{\varepsilon}^n \exp(-r\bar{\varepsilon}) \quad \text{or} \quad H(\bar{\varepsilon},T) = H(\bar{\varepsilon}) = K\bar{\varepsilon}^n \tag{9}$$

In forging process modeling, the decrease in the equivalent plastic flow stress with the temperature is often modeled [35,20] by the following terms:

$$\tau(T) = \exp(-\beta T) \quad \text{or} \quad \tau(T) = \exp(\beta/T) \tag{10}$$

Figures 13(*a*) and 13(*b*) show, respectively, the evolutions of $\ln(\bar{\sigma}_{est}^{max})$ versus the temperature T_i and versus the inverse of temperature $1/T_i$, where $\bar{\sigma}_{est}^{max}$ is the average of the maximal estimated stresses to each temperature T_i at both test velocities $V=3\times10^{-4}$ m s^{-1} and 3×10^{-2}m s^{-1}. As we can see on these figures, the evolution of $\ln(\bar{\sigma}_{est}^{max})$ as a function of the temperature or the inverse of temperature does not vary linearly. The mathematical formulations Eq. (10) seem not to be well appropriate to describe the evolution of the equivalent plastic stress versus temperature. Another formulation is then chosen differentiating the initial temperature T_{init} (298 K, 473 K, and 673 K) from the increased temperature ΔT due to the dissipation of the plastic deformation energy

$$\tau(T) = \tau_1(T_{init}) \cdot \tau_2(\Delta T) \quad \text{with } \Delta T = T - T_{init} \tag{11}$$

where

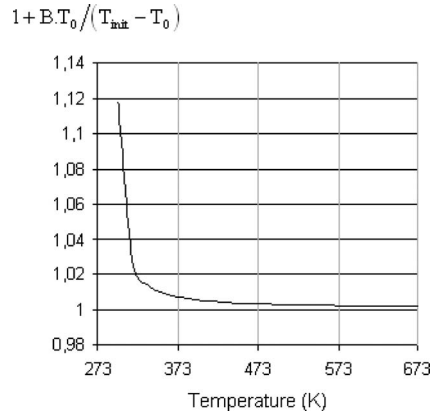

Fig. 14 Influence of the initial temperature on maximal estimated stress

$$\tau_1(T_{init}) = 1 + B \cdot T_0/(T_{init} - T_0) \quad \text{with } T_0 = 293 \text{ K} \tag{12}$$

and

$$\tau_2(\Delta T) = 1 - C \cdot (T - T_{init}) \tag{13}$$

Figure 14 presents the calculated value of the term $\tau(T_{init}) = 1 + B \cdot T_0/(T_{init} - T_0)$ as a function of the initial temperature T_{init}. The proposed formulation of the term $\tau_1(T_{init})$ allows us to model both the decrease in the equivalent plastic stress from ambient temperature to 473 K and remains constant between 473 K and 673 K. A linear decreasing function of the temperature is considered for the term $\tau_2(\Delta T)$. The proposed formulation of the term $\tau_1(T_{init})$ allows us to model both the decrease in the equivalent plastic stress from ambient temperature to 473 K and remains constant between 473 K and 673 K.

Finally, the two constitutive relationships

$$\bar{\sigma} = K \cdot \bar{\varepsilon}^n \exp(-r \cdot \bar{\varepsilon})[1 + B \cdot T_0/(T_{init} - T_0)](1 - C \cdot (T - T_{init})) \tag{14}$$

and

$$\bar{\sigma} = K \cdot \bar{\varepsilon}^n [1 + B \cdot T_0/(T_{init} - T_0)](1 - C \cdot (T - T_{init})) \tag{15}$$

respectively, called law I and law II are identified. Based on the complete experimental database presented in Fig. 9 and a FE model of the compression test, an inverse procedure of identification is carried out to determine the set of material parameters $P = \{K, n, r, B, C\}$. The software package FORGE2® dedicated to FE simulations of forming applications is used to simulate the com-

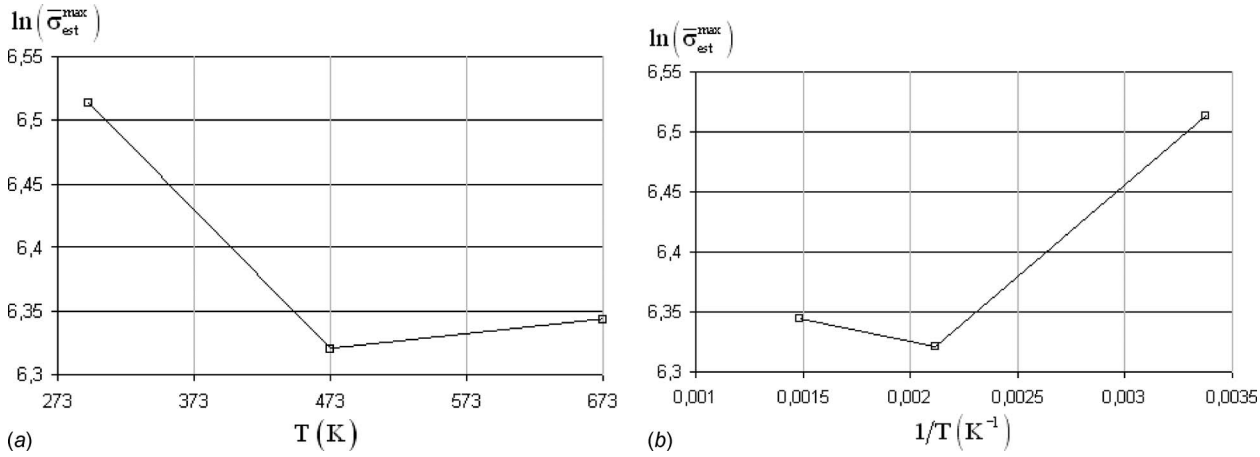

Fig. 13 Evolution of $\ln(\bar{\sigma}_{est}^{max})$ with (*a*) the temperature *T* and (*b*) the inverse of temperature $1/T$

Downloaded From: http://materialstechnology.asmedigitalcollection.asme.org/ on 09/29/2013 Terms of Use: http://asme.org/terms

Table 5 Identification results of the constitutive law parameters

		K (MPa)	n	r	B	C (K^{-1})	f (%)
Law I	Initial	723.86	0.20463	—	2.054×10^{-3}	1×10^{-3}	11.40
	Final	783.243	0.178183	—	1.8563×10^{-3}	7.8522×10^{-4}	4.64
Law II	Initial	783.243	0.178183	0.17	1.8563×10^{-3}	7.8522×10^{-4}	8.02
	Final	939.237	0.236078	0.295369	1.8685×10^{-3}	5.7029×10^{-4}	4.09

pression tests of specimens. The identification procedure used in the present work [24] is based on a gradient Gauss–Newton algorithm to solve the optimization problem. Of course, the gradient method does not ensure finding the global minimum but only a local one. In order to avoid these problems, the initial values of the constitutive law parameters P_{init} are determined by a regression method using the classical analytical compression test model (Sec. 1, Eqs. (1)–(3)) and the estimated stress $\bar{\sigma}_{\text{est}}$ versus estimated strain $\bar{\varepsilon}_{\text{est}}$ curves (Fig. 10), which constitute the experimental database. Then, the best set of parameters P_{init} is obtained by means of the inverse procedure minimizing the difference in a least-squares sense between the experimental forces versus displacement curves and the finite element calculated ones .

The identification results for the proposed constitutive equations are given in Table 5. The comparison of the cost function obtained from laws I and II at the end of the identification stage shows the interest of considering a structural softening sensitivity to determine the constitutive parameters. The comparison between the experimental and calculated (from law I) loads versus displacements curves is presented in Fig. 15. The compressive tests have been modeled for the six operating conditions corresponding to the experiments realized, i.e., three initial temperatures: 298 K, 473 K, and 673 K and two initial strain rates: 5×10^{-2} s^{-1} and 5 s^{-1} corresponding, respectively, to 3×10^{-4} m s^{-1} and 3×10^{-2} m s^{-1} impactor velocities. The friction coefficient value used in the FE simulation is 0.13. We can observe good agreement between the real and the predicted behavior: A global deviation of 4.09% is obtained from the constitutive law identified.

6 Conclusion

In order to characterize the material behavior at operating conditions encountered in forming applications, a new specimen shape has been proposed to realize uniaxial compression tests.

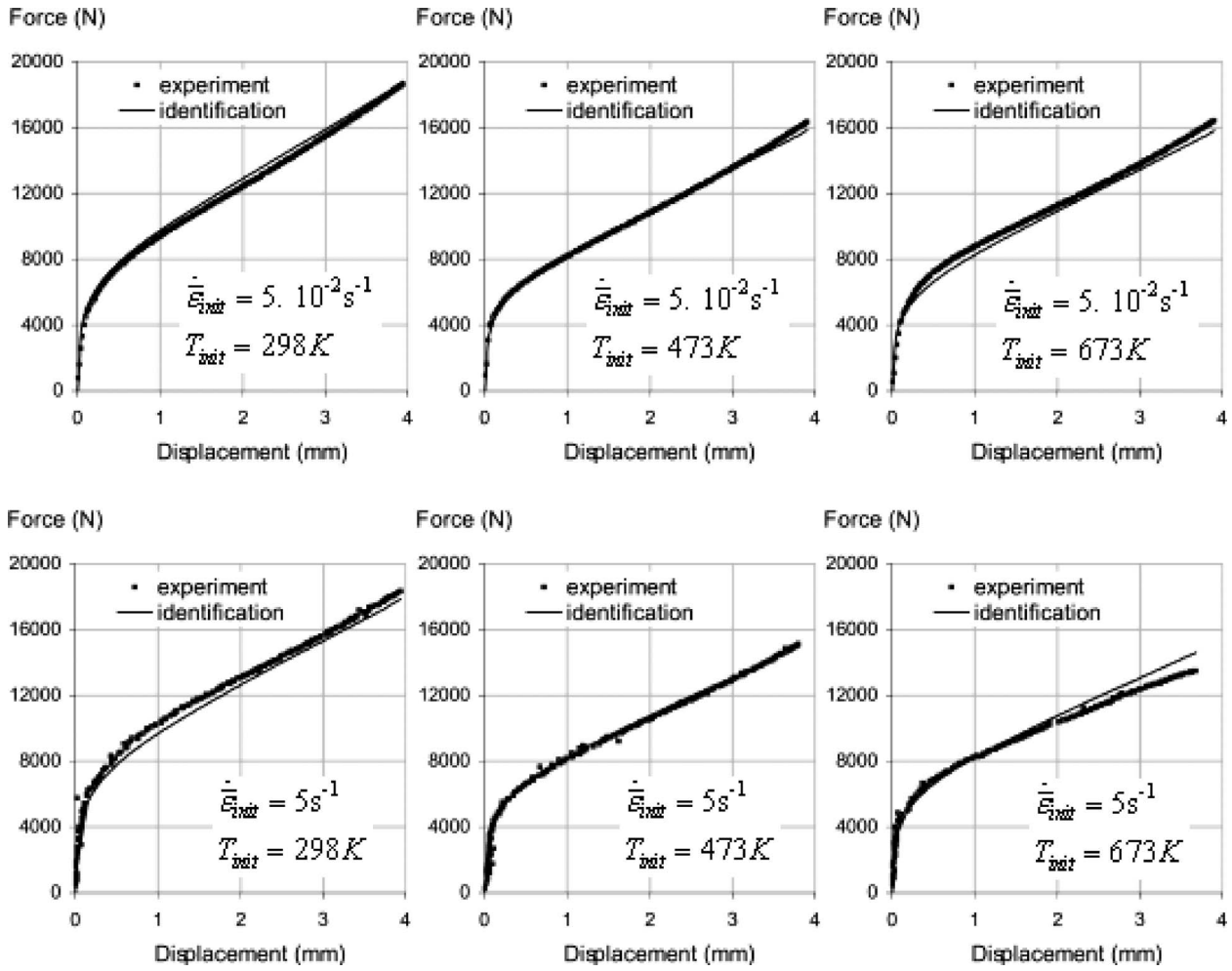

Fig. 15 Comparison between experimental and simulated forces versus displacement curves

Downloaded From: http://materialstechnology.asmedigitalcollection.asme.org/ on 09/29/2013 Terms of Use: http://asme.org/terms

Numerical investigations lead by means of the FE model of the compression test have shown the independence of both the load versus displacement curves and strain, strain rate, and temperature fields in the central part of the dumbbell specimen from the friction between the specimen and the dies. Moreover, this specimen shape allows us to avoid a too important overload on the load sensor when dynamic tests are considered. The pseudo-experimental validation has confirmed the independence of the rheological parameter determination from the friction coefficient considered at the interface between the tools and the specimen faces and has demonstrated the relevance of the proposed specimen shape. Finally, compression tests have been realized on 50CrMo4 steel at different temperatures and strain rates. Two mathematical formulations of constitutive relationships have been discussed. Starting from the experimental base, the material parameters of the proposed constitutive laws have been identified by means of an inverse procedure coupling a FE model of the compression test and an optimization tool minimizing the deviation between the experimental and calculated force versus displacement curves.

References

[1] Meyer, L. W., Halle, T., Herzig, N., Krüger, L., and Razorenov, S. V., 2006, "Experimental Investigations and Modelling of Strain Rate and Temperature Effects on the Flow Behavior of 1045 Steel," J. Phys. IV, **134**, pp. 75–80.

[2] Tanimura, S., Hayashi, H., and Yamamoto, T., 2006, "A Practical Constitutive Model Covering a Wide Range of Strain Rates and a Large Region of Strain," J. Phys. IV, **134**, pp. 55–61.

[3] Diot, S., 2003, "Caractérisation Expérimentale et Numérique du Comportement Dynamique des Matériaux," Ph.D. thesis, Institut National des Sciences Appliquées de Rennes, France.

[4] Kajberg, J., Sundin, K. G., Melin, L. G., and Stahle, P., 2004, "High Strain-Rate Tensile Testing and Viscoplastic Parameter Identification Using Microscopic High-Speed Photography," Int. J. Plast., **20**, pp. 561–575.

[5] Diot, S., Gavrus, A., Guines, D., and Ragneau, E., 2002, "Identification of a Forging Steel Behavior From Dynamic Compression Test," *Proceedings of the 15th ASCE Engineering Mechanics Conference, EM2002*, Columbia University, New York, NY, Jun. 2–5.

[6] François, D., 2001, *Essais Mécaniques et Lois de Comportement*, Editions Hermès Sciences, Paris.

[7] Van Rooyen, G. T., and Backoffen, W. A., 1960, "A Study of Interface Friction in Plastic Compression," Int. J. Mech. Sci., **1**, pp. 1–27.

[8] Oh, S. I., and Kobayashi, S., 1975, "An approximate method for a three dimensional analysis of rolling," Int. J. Mech. Sci., **17**(4), pp. 293–305.

[9] Gelin, J. C., Oudin, J., and Ravalard, Y., 1981, "Determination of the Flow Stress-Strain Curves for Metals From Axisymmetric Upsetting," J. Mech. Work. Technol., **6**, pp. 297–308.

[10] Kunogi, M., 1956, "A New Method of Cold Extrusion," J. Sci. Res. Inst. (Tokyo), **50**, pp. 215–246.

[11] Male, A. T., and Cockcroft, M. G., 1964, "Coefficient of Friction Under Condition of Bulk Plastic Deformation," J. Inst. Met., **93**, pp. 38–46.

[12] Avitzur, B., 1964, "Forging of Hollow Discs," Isr. J. Technol., **2**(3), pp. 295–304.

[13] Gorham, D. A., Pope, P. H., and Cox, O., 1984, "Sources of Error in Very High Strain Rate Compression Tests, Mechanical Properties at High Rates of Strain," *Proceedings of the Third Conference on the Mechanical Properties of Materials at High Rates of Strain*, Oxford, Apr. 9–12, Institute of Physics, UK, Conference series Vol. 70, pp. 151–158.

[14] Walley, S. M., Church, P. D., Furth, M., and Field, J. E., 1997, "A High-Speed Photographic Study of the Rapid Deformation of Metal Annuli: Comparison of Theory With Experiment," J. Phys. IV **7**(C3), pp. 317–322.

[15] Male, A. T., and De Pierre, V., 1970, "The Validity of Mathematical Solutions for Determining Friction From the Ring Compression Test," ASME J. Lubr. Technol., **39**, pp. 389–397.

[16] Rao, K. P., and Sivaram, K., 1993, "A Review of Ring-Compression Testing and Applicability of the Calibration Curves," J. Mater. Process. Technol., **37**, 295–318.

[17] Liu, J. Y., 1972, "An Analysis of Deformation Characteristics and Interfacial Friction Conditions in Simple Upsetting of Rings," ASME J. Eng. Ind., **94**(4), pp. 1149–1156.

[18] Lee, C. H., and Altan, T., 1972, "Influence of Flow Stress and Friction upon Metal Flow in Upset Forging of Rings and Cylinders," ASME J. Eng. Ind., **94**(3), 775–782.

[19] Hwu, Y., Hsu, C., and Wang, F., 1993, "Measurement of Friction and the Flow Stress of Steels at Room and Elevated Temperatures by Ring-Compression Tests," J. Mater. Process. Technol., **37**, pp. 319–335.

[20] Kopp, R., Luce, R., Leisten, B., Wolskz, M., Tschirnich, M., Rehrmann, T., and Volles, R., 2001, "Flow Stress Measuring by Use of Cylindrical Compression Test and Special Application to Metal Forming Processes," Steel Res., **72**(10), pp. 394–401.

[21] Kopp, R., Heuben, J. M. M., Philipp, F. D., and Karhausen, K., 1993, "Improvement of Accuracy in Determining Flow Stress in Hot Upsetting Tests," Steel Res., **64**(8/9), pp. 377–384.

[22] Mataya, M. C., and Sackschewsky, V. E., 1994, "Effect of Internal Heating During Hot Compression on the Stress-Strain Behavior of Alloy 304L," Metall. Mater. Trans. A, **25A**, pp. 2737–2752.

[23] Parteder, E., and Bünten, R., 1998, "Determination of Flow Curves by Means of a Compression Test Under Sticking Friction Conditions Using an Iterative Finite-Element Procedure," J. Mater. Process. Technol., **74**, pp. 227–233.

[24] Gavrus, A., 1996, "Identification Automatique des Paramètres Rhéologiques par Analyse Inverse," Ph.D. thesis, Ecole Nationale Supérieure des Mines de Paris, CEMEF, Sofia Antipolis, France.

[25] Dal Negro, T., D'Alvise, L., Chastel, Y., and Massoni, E., 2001, "Inverse Technique for Automatic Identification of Rheological Parameters in Combined Tension-Torsion and Compression," *Proceedings of ESAFORM 2001*, Liège, pp. 419–422.

[26] Szyndler, D., Pietrzyk, M., and Kusiak, R., 2001, "Estimation of Rheological and Friction Parameters in Hot Forming Processes as Inverse Problem," *Proceedings of ESAFORM 2001*, Liège pp. 191–194.

[27] Szeliga, D., Matuszyk, P., Kusiak, R., and Pietrzyk, M., 2002, "Identification of Rheological Parameters on the Basis of Various Types of Plastometric Tests," J. Mater. Process. Technol., **125–126** pp. 150–154.

[28] Gavrus, A., Ragneau, E., and Guines, D., 2002, "Identification of the Friction Coefficients Directly From a Forging Process," *Proceedings of Euromech 435, Friction and Wear in Metal Forming*, Jun. 18–20, pp. 125–132, Valenciennes, France.

[29] François, D., 1996, *Essais Mécaniques des Métaux–Détermination des Lois de Comportement*, Vol. MB2, Les Techniques de l'Ingénieur, Paris, France.

[30] Nagamatsu, A., Murota, T., and Jimma, T., 1971, "On the Non-Uniform Deformation of Material in Axially Symmetric Compression Caused by Friction, Part One," Bull. JSME, **14**(70), pp. 331–338.

[31] Nagamatsu, A., Murota, T., and Jimma, T., 1971, "On the Non-Uniform Deformation of Material in Axially Symmetric Compression Caused by Friction, Part Two," Bull. JSME, **14**(70), pp. 339–347.

[32] Kobayashi, S., Oh, S. I., and Altan, T., 1989, *Metal Forming and the Finite Element Method*, Oxford University Press, New York.

[33] Deltort, B., Neme, A., and Tanguy, B., 1997, "A New Geometry for Compression Hopkinson Bars," J. Phys. IV, **7**, pp. 265–270.

[34] FORGE2®, Centre de Mise en Forme de Matériaux (CEMEF), Transvalor S.A, BO037, Sophia-Antipolis, France.

[35] Hamdi, R., 1997, "Comportement Quasi-Statique et Dynamique des Aciers Pour Frappe et Forge à Froid," Ph.D. thesis, Université de Technologie de Compiègne, France.

[36] Stevenson, R., 1981, "A comparison of constitutive relations incorporating strain rate hardening," J. Eng. Mater. Technol., Technical briefs, **103**, pp. 261-263.

[37] Symonds, P. S., 1967, "Survey of Methods of Analysis for Plastic Deformation of Structures Under Dynamic Loading," BU/NSRDC, Brown University, Report No. BU/NSRDC.

[38] Johnson, R., and Cook, W. H., 1983, "A Constitutive Model and Data for Metal Subjected to Large Strains, High Strain Rates and High Temperatures," *Proceedings of the Seventh International Symposium on Ballistics*, The Hague, The Netherlands, pp. 541–547.

[39] Gavrus, A., Ragneau, E., and Caestecker, P., 2003, "Analysis of a Constitutive Model for the Simulation of Dynamic Forming Processes," Int. J. Form. Processes, **6**(1), pp. 33–52.

[40] Kang, W. J., Cho, S. S., Huh, H., and Chung, D. T., 1999, "Modified Johnson-Cook model for vehicle body crashworthiness simulation," Int. J. Veh. Des., **21**(4/5), pp. 424–435.

[41] Langrand, B., Geoffroy, P., Petitniot, J.-L., Fabis, J., Markiewicz, E., and Drazetic, P., 1999, "Identification technique of constitutive model parameters for crashworthiness modelling," Aerosp. Sci. Technol., **3**(4), pp. 215–227.

[42] Liang, R. and Khan, A. S., 1999, "A critical review of experimental results and constitutive models for BBC and FCC metals over a wide range of strain rates and temperatures," Int. J. Plast. (15), pp. 963–850.

[43] Homquist, T. J., and Johnson, G. R., 1991, "Determination of Constants and Comparison of Results for Various Constitutive Models," J. Phys. IV, **1**(8), pp. 853–860.

[44] Meyer, L. W., Seifert, K., and Abdel-Malek, S., 1997, "Behavior of Quenched and Tempered Steels Under High Strain Rate Compression Loading," J. Phys. IV, **7**(8), pp. 571–576.

[45] Zerilli, F. J., and Armstrong, R. W., 1987, "Dislocations Mechanics Base Constitutive Relations for Material Dynamic Calculations," J. Appl. Phys., **61**(5), pp. 1816–1825.

[46] Valentin, T., Magain, P., Quik, M., Labibes, K., and Albertini, C., 2000, "Validation of Constitutive Equations for Steel," J. Phys. IV, **7**(3), pp. 611–616.

[47] Lei, W., Yao, M., and Chen, B., 1996, "Quantitative Description of Temperature and Strain Rate Dependence of Yield Strength of Structural Steels," Eng. Fract. Mech., **53**(4), pp. 643–663.

[48] Majta, J., Zurek, A., Trujillo, C., and Bator, A., 2003, "Study of High Strain Rate Plastic Deformation of Low Carbon Microalloyed Steels Using Experimental Observation and Computational Modelling," J. Phys. IV, **110**, pp. 117–122.

[49] Cabrera, J. M., Prado, J. M., and Barron, M. A., 1999, "An Inverse Analysis of the Hot Uniaxial Compression Test by the Means of the Finite Element Method," Steel Res., **70**, pp. 59–66.

Downloaded From: http://materialstechnology.asmedigitalcollection.asme.org/ on 09/29/2013 Terms of Use: http://asme.org/terms